Preparation of Graphene-Multi-Walled Carbon Nanotube Composite for Quantitive Determination of 2-hydroxy-3-Methylanthraquinone in *Hedyotis diffusa*

Zheng Wei[1][#], Junping Zhang[1][#], Xiaohe He[2], Shufang Ma[1], Aihua Zhang[1], Weifeng Cui[1], Yafeng Li[1], Xiaoping Cai[1], Shuibao Zhang[2], Junming Fan[1,]*

[1] Henan Academy Institute of Traditional Chinese Medicine, Zhengzhou, 450000, Henan, P. R. China
[2] Henan University of Chinese Medicine，Zhengzhou, 450000, Henan, P. R. China
[#] These authors contributed equally to this work
[*]E-mail: junmingfan@yeah.net

In this study, an electrochemical sensor based on a novel composite of reduced graphene oxide (GO) and multi-walled carbon nanotube (CNT) was developed for the detection of 2-hydroxy-3-methylanthraquinone. First, GO was employed to disperse CNT as a dispersant. Then GO was reduced electrochemically into RGO after being deposited on the surface of ITO. Thus, the designed electrochemical sensor based on RGO/CNT/ITO for detecting 2-hydroxy-3-methylanthraquinone was first reported. Cyclic voltammetry and electrochemical impedance spectroscopy (EIS) were employed to analyse the sensor. The results indicated that the sensor exhibited an electrocatalytic activity for the reduction of 2-hydroxy-3-methylanthraquinone. In particular, the electrochemical reduction of 2-hydroxy-3-methylanthraquinone was remarkably enhanced by the RGO/CNT composite. Besides, the sensor was efficient in determining 2-hydroxy-3-methylanthraquinone in *Hedyotis diffusa*, where the sensor exhibited a linear response range from 2 to 600 μM.

1. INTRODUCTION

The herb of *Hedyotis diffusa Willd* (*H. diffusa*), a member of Rubiaceae with a synonym of *Oledenlandia diffusa Willd*, is an annual herb located at Northeast Asia. It has been recognized as a conventional oriental medicine to cure sore throat, tonsillitis, hepatitis, appendicitis, urethral infection and cancer [1]. In recent years, *H. diffusa Willd* has been applied in clinic for a positive treatment of various cancers. So far, three main categories of the compounds from this herb, such as anthraquinone,

polysaccharide and triterpene, have been demonstrated to be bioactive [2]. Besides, two anthraquinones, which have been discovered and isolated from the extract of *H. diffusa Willd* with water, exhibits apoptosis-inducing effect against the cancel cells [3]. The inhibition of apoptosis, which is a common and effective cellular suicide approach, have considered as one of the characteristics of cancer [4]. Thus, the introduction of specific apoptosis with selectivity into the tumor cells becomes a primary object of cancer therapy [5, 6]. Majority of the treatments employed currently target in one or other way of apoptosis of tumor cells [7]. Phosphorylation can regulate the activity of the class of the mitogen-activated protein kinase (MAPK), including p38, C-Jun N-terminal kinase (JNK) and extracellular-signal-regulated kinase (ERK) [8, 9]. In general, the activation of both JNK and p38 could promote apoptosis. However, due to the transduction of survival signals, ERK acts as the anti-apoptotic molecules [10]. Besides, under some definite conditions, the pro-survival effects including LPS-induced activation of BV-2 cells have been observed in p38 or JNK. Caspases, which belong to the class of proteases, are essential for the apoptotic approach, where they have been recognized as the promotor for apoptosis [11, 12]. It has been reported that a variety of stimuli could cause apoptosis in diverse kinds of cells. Two anthraquinones from *H. diffusa* have been reported by Shi et al. that they can cause HepG2 Cell apoptosis through caspase-3 activation [13]. Methylanthraquinone extracted from *H. diffusa Willd* have been demonstrated recently that it can result in the Ca^{2+}-mediated apoptosis in human breast cancer cells [14]. Nevertheless, the molecular mechanisms for the apoptosis induced by *H. diffusa Willd* are ambiguous, in particular for human leukemic cells. The cell growth suppression of leukemia cells is investigated with the U937 tumor cells which are a potential model through physical, chemical and physiological agents. The direct activation of MAPK is assumed to play an essential role in 2-hydroxy-3-methylanthraquinone for the *H. diffusa Willd*-induced apoptosis in U937 cells. Thus, the development of the facile and inexpensive approaches with high accuracy becomes crucial for the determination of in the herb specimens.

Electrochemical methods, which are useful and versatile analytical approaches, exhibited the characteristics of relatively low cost, high accuracy and sensitivity and wide linear dynamic range. The electroanalytical measurements are widely applied in the drug analysis for their dosage forms, especially for the biological specimens, when more sensitive pulse techniques have been developed. Numerous issues of the pharmaceutical interest could be resolved with the electroanalytical methods with high level of sensitivity, selectivity, precision and accuracy.

Carbon nanotubes have been extensively employed to fabricate the electrochemical sensors, because of their distinct properties, such as high level of flexibility, strength, electrical and thermal conductivity [15-23]. Hence, CNT as the significant species have employed to generate a composite with other materials so that to improve the electrocatalytic performance of the electrode. For instance, a polypyrrole-imprinted electrochemical sensor for determining oleanolic acid, which was fabricated with the carbon electrode modified by the SnO_2-CNT composite, was reported by Zhang and co-workers. Moreover, graphene, which is a kind of two-dimensional sp2-hybridized carbon material, has extensive interests of numerous research groups, due to its low cost, outstanding charge transport mobility, high specific surface area and electrocatalytic activity [24-27]. Thus, graphene has been applied in sensing as a novel carbon-based electrocatalysts. Consequently, we attempted to develop a proper electrode material through combining graphene and CNT for the detection of 2-hydroxy-3-

methylanthraquinone. Herein, a novel sensor was fabricated to detect 2-hydroxy-3-methylanthraquinone, which was based the ITO modified with the composite of CNT and RGO. An outstanding performance was observed with the designed sensor for detecting 2-hydroxy-3-methylanthraquinone ions in *H. diffusa* samples.

2. EXPERIMENTS

2.1. Materials

Synthetic graphite with a mean particle size of below 20 μm was commercially available (Sigma-Aldrich). CNT with a diameter of 40-60 nm and a length of 1-2 μm (purity ≥ 95%) was obtained from Shenzhen Nanotech Port Co. Ltd (China). 2-hydroxy-3-methylanthraquinone was purchased from Hean technology company (Shanghai, China). All the other chemicals were analytically pure and used without any purification. For all the experiments, Milli-Q water (18.2 MΩ cm) was employed.

2.2. Preparation of CNT-RGO

The Hummers' method with a few modifications was employed to synthesize graphene oxide [28, 29]. To prepare the dispersion of MWCNT in GO, GO (80 mg) was added into water (160 mL) with ultrasonic irradiation for 1 h under ambient condition. Then CNT (20 mg) was added into the as-prepared dispersion and under ultrasound for another 3 h, where a black homogeneous suspension was obtained. Subsequently, MWCNT-GO dispersion (1 mL) was deposited onto the ITO substrate and dried at room temperature.

The electrochemical reduction of MWCNT-GO into MWCNT-RGO was carried out, where a traditional three-electrode system was employed. In this work, the MTCNT-GO/ITO was used as the working electrode, while the platinum wire and Ag/AgCl with KCl (3M) were employed as the auxiliary electrode and reference electrode. For the preparation of MWCNT-RGO/ITO with the electrochemical reduction approach, MWCNT-GO-ITO was immersed into PBS solution (pH 7.0) with a concentration of 0.1 M through the cyclic sweeping with a potential in the range of 0 to -1.4 V for 10 cycles, where the scanning rate was 10 mV/s.

2.3. Characterizations

Scanning electron microscopy (SEM, S-4700, Hitachi High Technologies Corporation) was employed to characterize the morphology of the MWCNT-RGO film. An optical 3D profiler (Contour GT-I, Bruker) was used to measure the thickness of the film. FTIR spectra were recorded with FTIR spectrometer (Nicolet 8700, Thermo Scientific Instrument). Besides, UV-Vis spectrometer (Perkin Elmer Lambda 950) was employed to perform the optical analysis.

2.4. Electrochemical determination

CHI430A electrochemical working station with a three-electrode system was employed to perform all the electrochemical measurements. Ag/AgCl, Pt wire and CNT/RGO/ITO were used as the reference electrode, auxiliary electrode and working electrode, respectively. The resistance performance of the electrode was characterized through electrochemical impedance spectroscopy, where $[Fe(CN)6]^{3-/4-}$ (5 mM) and KCl (0.1 M) acted as probe and supporting electrolyte respectively. The frequency range was set to be 10^1 to 10^5 Hz, while the amplitude was settled to be 5 mV. The electrochemical determination of 2-hydroxy-3-methylanthraquinone was carried out in PBS with a concentration of 0.1 M through the CV approach, where the scanning range was -0.7 to -1.5 V with a scanning rate of 50 mV/s. Similarly, the DPV measurements were also performed at the scanning range from -0.7 to -1.5 V. Besides, the modulation time was set to be 0.05 s with a time interval of 0.2 s, while the step potential was 0.5 mV/s.

3. RESULTS AND DISCUSSION

SEM was employed to characterize the morphology of the CNT-RGO film. The top-view SEM images of the CNT-RGO film with various magnification were illustrated in Figure 1. It was obvious that CNT and RGO sheets exhibited a remarkably compact structure. Besides, a homogeneous surface morphology was observed in the thin film of the fabricated composite.
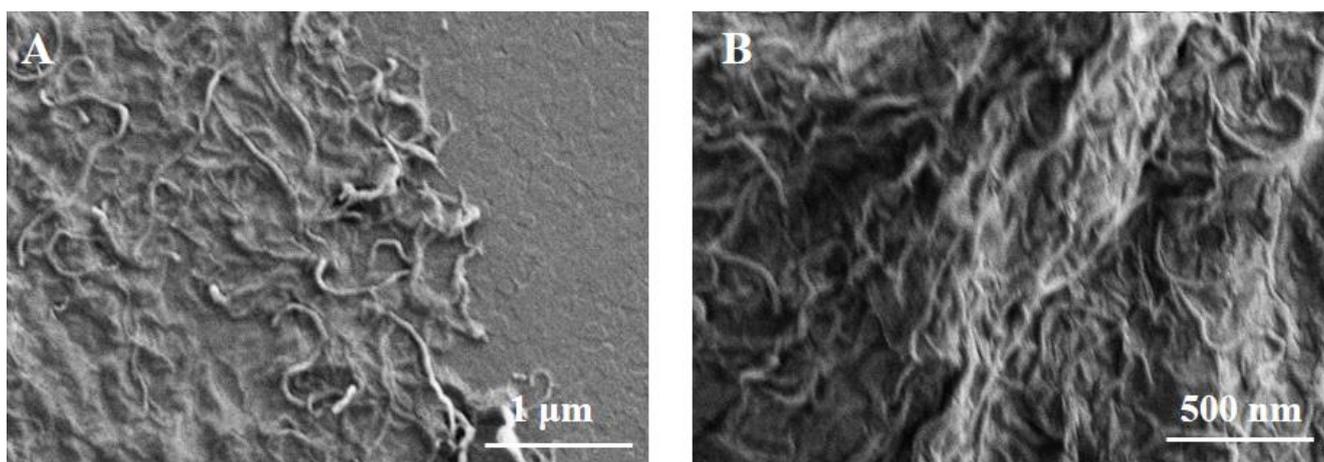
Figure 1. SEM image of the CNT-RGO composite in (A) low magnification and (B) high magnification.

To confirm the reduction process during the CV scanning, UV-Vis spectroscopy was employed. The UV-Vis spectra of GO and CNT-RGO were clarified in Figure 1A. Two characteristic adsorption peaks were observed at 225 and 317 nm as expected, which were ascribed to the π—π* transitions of aromatic C—C bonds and the n—π* transitions of C=O bonds, respectively [30]. In

comparison, for MWCNT-RGO, the peak at 225 nm which was attributed to GO exhibited a red shift to 266 nm, while a shoulder adsorption peak which presented in the spectrum of GO disappeared. The results indicated that GO was reduced during the CV scanning. The geometric wrinkling not only minimizes the surface energy but also induces mechanical integrity with high Young's modulus, tensile strength, and good film-forming ability, due to nanoscale sheet interlocking [31].

FTIR was used to further confirm the reduction process. The FTIR spectra of CNT-GO and CNT-RGO were shown in Figure 2B. It was obvious that several characteristic peaks at 3430, 1636, 1171 and 1042cm^{-1} were observed in the spectra of CNT-GO, which were attributed to the stretching vibration of ─OH, carboxyl C=O, epoxy C─O and alkoxy C─O, respectively [32]. Therefore, reduction of GO to RGO provided us with a material having reduced number of carboxylic acid, ether, and hydroxyl groups. This decreased D band intensity in Raman spectroscopy; however it has various effects with matrix compatibility, mostly positive [33, 34]. However, according to the spectrum of CNT-RGO, the intensity of these peaks decreased significantly even vanished after CV scanning, which confirmed the formation of RGO.
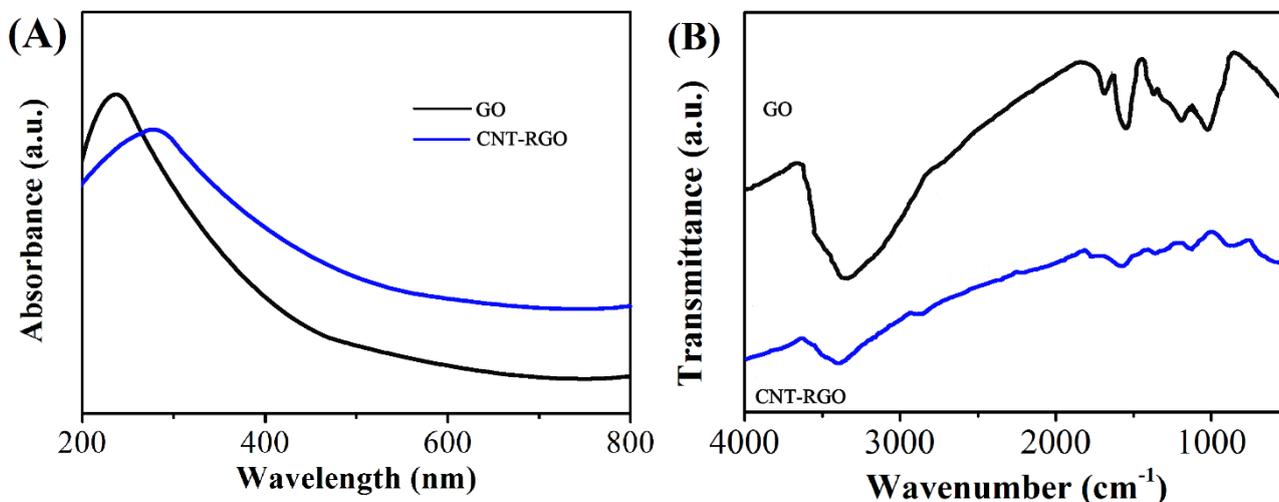
Figure 2. (A) UV-vis spectra of GO and CNT-RGO. (B) FTIR spectra of CNT-GO and CNT-RGO.

Electrochemical impedance spectroscopy (EIS) was employed to analyze the differences in the electrochemical capacity of ITO with and without modification. The EIS curves of the bare ITO, RGO/ITO and CNT-RGO/ITO with [Fe(CN)$_6$]$^{3-/4-}$ solution (5 mM) were clarified in Figure 3. It was obvious that the EIS curves exhibited two parts including the semicircular and the straight line. The semicircular represented the electron transfer limited process status of the electrode, where the diameter equaled to the value of the electron transfer resistance. However, the straight line meant the diffusion process status of the electrode. For the bare ITO, a relatively larger semicircular was observed with a straight line. In the case of RGO/ITO, the modified ITO exhibited even bigger semicircular than the bare ITO, which indicated that the electron transfer was suppressed by the modification with RGO. This phenomenon was induced by the oxygen-based groups present on the surface of ITO, which hindered the electron transfer of ferri/ferro cyanide [35]. On the contrary, the

CNT-RGO/ITO exhibited a significantly smaller semicircular, which indicated that the resistance of the electron transfer to the redox-probe which was dissolved in the electrolyte was remarkably low. Thus, the electrochemical capacity of the electrode was significantly enhanced by adding the CNT. Similar results have been observed by other researchers as well [36-38].
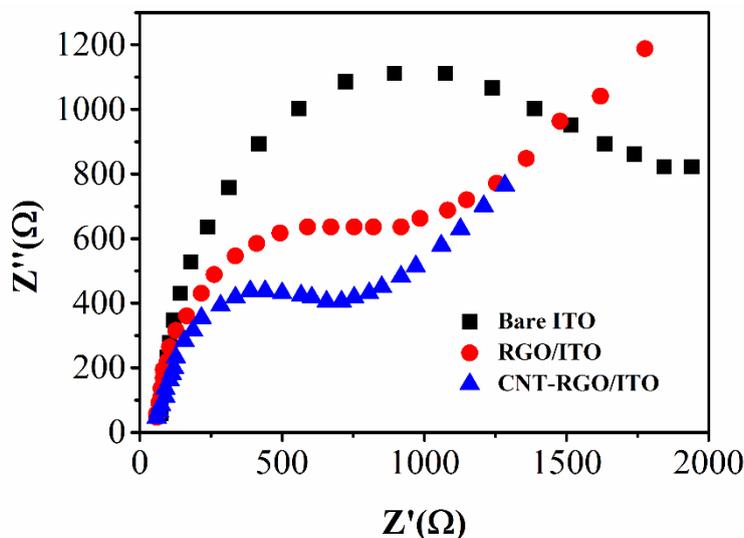
Figure 3. Nyquist plots of the bare ITO, RGO/ITO and CNT-RGO/ITO in $K_4[Fe(CN)_6]$ (5 mM) with KCl (0.1 M).
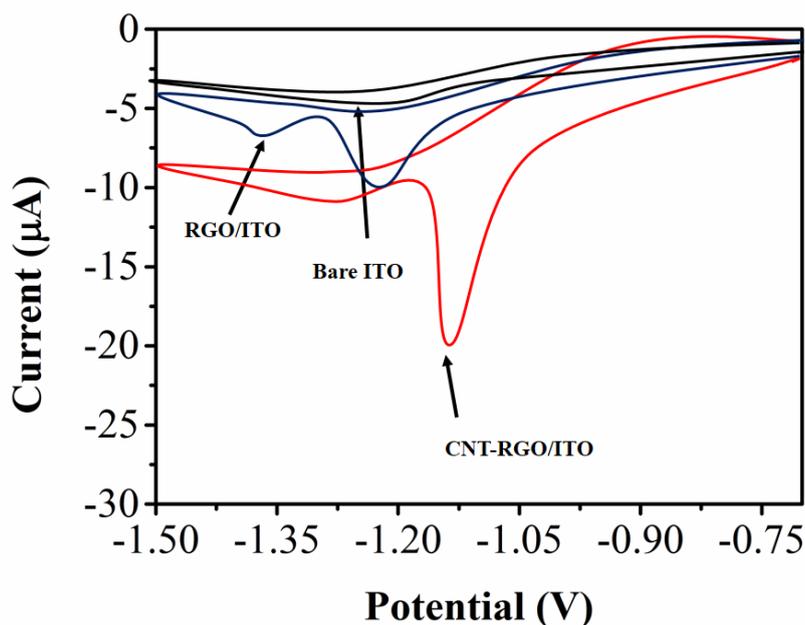
Figure 4. Cyclic voltammograms of the bare ITO, RGO/ITO and CNT-RGO/ITO toward 2-hydroxy-3-methylanthraquinone in PBS with a concentration of 100 μM, where the scan rate was 50 mV/s.

Figure 4 illustrated the cyclic voltammograms of 2-hydroxy-3-methylanthraquinone with a concentration of 100 M in PBS with various electrodes. A nonreversible response towards the

reduction of 2-hydroxy-3-methylanthraquione in the absence of the oxidation peaks was observed in all the bare ITO, RGO/ITO and CNT-RGO/ITO at the scanning range. Besides, for various electrode, the CV profiles exhibited remarkable differences. Compared to the bare ITO, the RGO/ITO possessed a higher electron transfer resistance.

However, because of the larger surface area of RGO, the reduction response was enhanced significantly at RGO/ITO, which indicated that the 2-hydroxy-3-methylanthraquinone molecules were efficiently absorbed resulting in a high signal. In addition, CNT-RGO/ITO exhibited a significantly higher current response, where the reduction potential (-1.12 V) shifted positively. Especially, no peak was observed, while no 2-hydroxy-3-methylanthraquione presented. Hence, the peak of -1.12 V were remarkably corresponding to the reduction of 2-hydroxy-3-methylanthraquinone.

The effect of the electrolyte was analyzed. Figure 5A illustrated the reduction values, where the response of the reduction of 2-hydroxy-3-methylanthraquinone reduction was collected at PBS with a concentration of 0.1 M, $Na_2C_2O_4$, H_2SO_4 and HAc-NaAc, respectively. It was obvious that the highest response was obtained with PBS towards the reduction of 2-hydroxy-3-methylanthraquinone. Hence, PBS was selected in this study. Thereafter, the effect of the pH value was analyzed. In Figure 5B, the peak current exhibited an elevation when increasing the pH value from 3 to 5.5. However, the peak current then decreased with further increasing the pH. Thus, pH 5.5 was selected as the optimum for further investigation. Besides, the relationship between the current response and the amount of the modifier was also investigated.
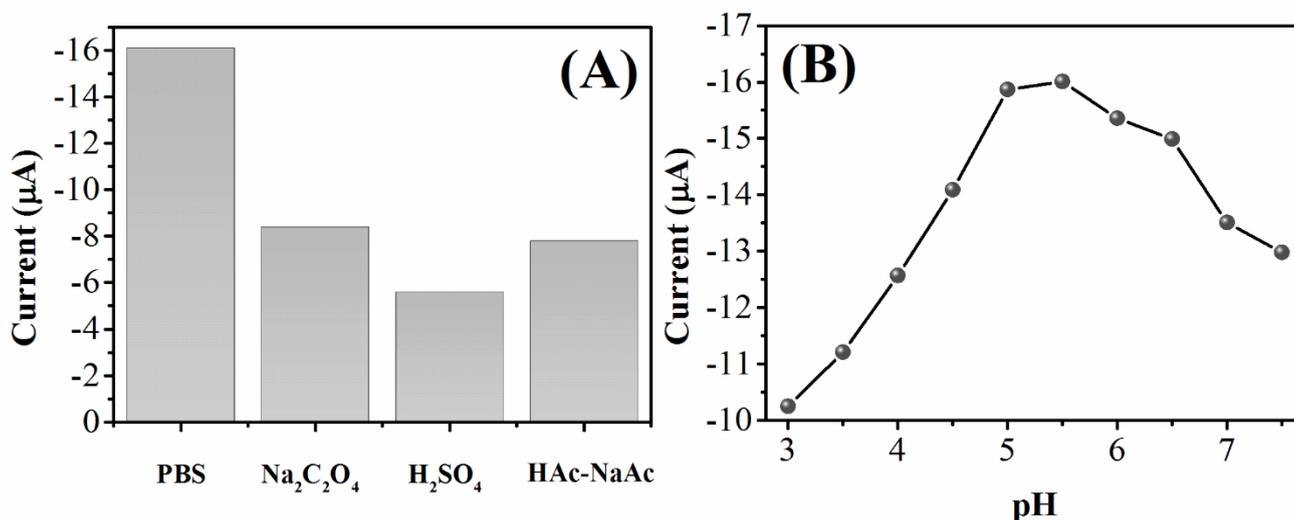
Figure 5. Influence of the electrolyte types (A) and the pH values of PBS (B) on the electrochemical reduction of 2-hydroxy-3-methylanthraquinone.

The differential pulse voltammetry (DPV) approach was employed to investigate the analytical capacity of the CNT-RGO/ITO under the optimized conditions. The DPV curves of the CNT-RGO/ITO towards 2-hydroxy-3-methylanthraquinone with various concentrations was illustrated in Figure 6. It was obvious that the current exhibited a proportional relationship with the concentration of 2-hydroxy-3-methylanthraquinone in the range of 2 to 600 μM, whereas a wider linear range of this

detection was observed than the previous reports. To our best knowledge, the determination of 2-hydroxy-3-methylanthraquinone was first reported.
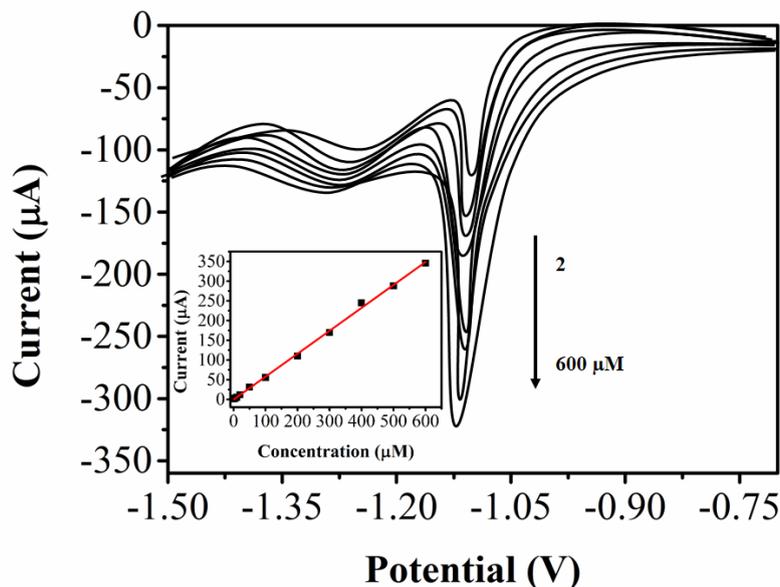
Figure 6. DPV curves of CNT-RGO/ITO towards 2-hydroxy-3-methylanthraquinone in PBS with various concentrations, where pH was 5.5. Inset: plots of the relationship between the reductive peak current and the concentration.

The detection of 2-hydroxy-3-methylanthraquinone with a concentration of 100 ☐M was used to test the reproducibility of the as-synthesized CNT-RGO/ITO, where ten electrodes which were freshly produced was employed. The relative standard deviation (RSD) was calculated to be 3.15%, indicating that the proposed electrochemical sensor for the detection of 2-hydroxy-3-methylanthraquinone exhibited a prominent reproducibility. The stability of the CNT-RGO/ITO was evaluated by performing the determination of 2-hydroxy-3-methylanthraquinone with a concentration of 100 μM for five times.

Table 1. Determination of the content of 2-hydroxy-3-methylanthraquinone in four extracting specimens of *H. diffusa* with CNT-RGO/ITO.

Sample	Addition (μM)	Found (μM)	Recovery (%)	RSD (%)
1	0	5.47	—	4.75
	10	15.56	100.58	3.66
2	0	4.96	—	5.21
	50	55.21	100.45	6.33
3	0	8.54	—	2.38
	10	18.02	97.19	4.69
4	0	13.55	—	3.41
	50	62.74	98.73	5.88

The current response of the designed CNT-RGO/ITO exhibited a decrease of 3.77%. Furthermore, the long-term storing stability of the CNT-RGO/ITO was evaluated, where the CNT-RGO/ITO was stored in fridge for one month. According to the current response, 96.4% of the original activity was still remained in the CNT-RGO/ITO after storing for one month.

The practical applicability of the designed CNT-RGO/ITO for the determination of 2-hydroxy-3-methylanthraquinone in real samples was evaluated, where four extracting specimens of grape fern herb were tested. Besides, the confirmation of the designed method was tested through employing the spike and recovery process. Table 1 clarified the measurement results of the designed electrochemical sensor. It was obvious that the designed CNT-RGO/ITO exhibited a remarkable capacity towards the detection of 2-hydroxy-3-methylanthraquinone in the extracting specimens of grape fern herb, which indicated that the proposed sensor was efficient for the determination of 2-hydroxy-3-methylanthraquinone detection in the pratical herb specimens.

4. CONCLUSIONS

In conclusion, a facile electrochemical reduction approach was employed to synthesize a novel composite of CNT and RGO, where the dispersion of CNT in GO was used as precursor. UV-Vis and FTIR spectroscopy was employed to characterize the sensor, which confirmed that the reduction was successfully completed during the CV scans. The designed sensor based on CNT-RGO/ITO was first applied with a reliable, sensitive and selectivity in determining 2-hydroxy-3-methylanthraquinone, which was extracted from the grape fern herb. Besides, a linear response range was obtained with the sensor between 2 and 600 μM.

References

1. G.-H. Xu, Y.-H. Kim, S.-W. Chi, S.-J. Choo, I.-J. Ryoo, J.-S. Ahn and I.-D. Yoo, *Bioorganic & medicinal chemistry letters*, 20 (2010) 513
2. C. Li, X. Xue, D. Zhou, F. Zhang, Q. Xu, L. Ren and X. Liang, *Journal of pharmaceutical and biomedical analysis*, 48 (2008) 205
3. L. Yu, Y. Li and X.-J. Guo, *Chroma*, 70 (2009) 211
4. C. Widmann, S. Gibson, M.B. Jarpe and G.L. Johnson, *Physiological reviews*, 79 (1999) 143
5. A. Brunet and J. Pouysségur, *Essays in biochemistry*, 32 (1996) 1
6. C. Yu, X. Mao and W. Li, *Biochemical and biophysical research communications*, 331 (2005) 391
7. S. Schneider-Jakob, N. Corazza, A. Badmann, D. Sidler, R. Stuber-Roos, A. Keogh, S. Frese, M. Tschan and T. Brunner, *Cell death & disease*, 1 (2010) e86
8. Y. Miyata and E. Nishida, *Biochemical and biophysical research communications*, 266 (1999) 291

9. L. Chang and M. Karin, *Nature*, 410 (2001) 37
10. Z. Xia, M. Dickens, J. Raingeaud, R.J. Davis and M.E. Greenberg, *Science*, 270 (1995) 1326
11. C.-F. Lin, Y.-H. Lo, M.-C. Hsieh, Y.-H. Chen, J.-J. Wang and M.-J. Wu, *Bioorganic & medicinal chemistry*, 13 (2005) 3565
12. C. Johnson and W. Jarvis, *Apoptosis*, 9 (2004) 423
13. Y. Shi, C.-H. Wang and X.-G. Gong, *Biological and Pharmaceutical Bulletin*, 31 (2008) 1075
14. Z. Liu, M. Liu, M. Liu and J. Li, *Toxicology in vitro*, 24 (2010) 142
15. S.S. Stavitskaya, V.M. Vikarchuk, M.F. Kovtun, O.I. Poddubnaya and A.M. Puziy, *J. Water Chem. Technol.*, 36 (2014) 110
16. M.M. Barsan, M.E. Ghica and C.M. Brett, *Anal. Chim. Acta.*, 881 (2015) 1
17. H. Dai, E.T. Thostenson and T. Schumacher, *Sensors*, 15 (2015) 17728
18. J. Muñoz, F. Cespedes and M. Baeza, *Microchemical Journal*, 122 (2015) 189
19. W. Lee, H. Koo, J. Sun, J. Noh, K.-S. Kwon, C. Yeom, Y. Choi, K. Chen, A. Javey and G. Cho, *Scientific reports*, 5 (2015)
20. L.H. Hsu, E. Hoque, P. Kruse and P.R. Selvaganapathy, *Applied Physics Letters*, 106 (2015) 063102
21. G.J. Gallo and E.T. Thostenson, *Materials Today Communications*, 3 (2015) 17
22. P. Sun, S.M. Bachilo, R.B. Weisman and S. Nagarajaiah, *The Journal of Strain Analysis for Engineering Design*, (2015) 0309324715597414
23. S. Lu, L. Bai, Y. Wen, M. Li, D. Yan, R. Zhang and K. Chen, *Journal of Solid State Electrochemistry*, 19 (2015) 2023
24. K.S. Novoselov, A.K. Geim, S.V. Morozov, D. Jiang, Y. Zhang, S.V. Dubonos, I.V. Grigorieva and A.A. Firsov, *Science*, 306 (2004) 666
25. S. Stankovich, D.A. Dikin, G.H.B. Dommett, K.M. Kohlhaas, E.J. Zimney, E.A. Stach, R.D. Piner, S.T. Nguyen and R.S. Ruoff, *Nature*, 442 (2006) 282
26. L. He, L. Fu and Y. Tang, *Catalysis Science & Technology*, (2015)
27. L. Fu and Z. Fu, *Ceram. Int.*,
28. W.S. Hummers and R.E. Offeman, *Journal of the American Chemical Society*, 80 (1958) 1339
29. T. Gan and S. Hu, *Microchim. Acta.*, 175 (2011) 1
30. J.I. Paredes, S. Villar-Rodil, A. Martínez-Alonso and J.M.D. Tascón, *Langmuir*, 24 (2008) 10560
31. Y. Xu, H. Bai, G. Lu, C. Li and G. Shi, *Journal of the American Chemical Society*, 130 (2008) 5856
32. Z. Liu, J.T. Robinson, X. Sun and H. Dai, *Journal of the American Chemical Society*, 130 (2008) 10876
33. P. Pokharel, *Chem. Eng. J.*, 253 (2014) 356
34. T. Kuilla, S. Bhadra, D. Yao, N.H. Kim, S. Bose and J.H. Lee, *Progress in polymer science*, 35 (2010) 1350
35. D.S. Jeykumari, S. Ramaprabhu and S.S. Narayanan, *Carbon*, 45 (2007) 1340
36. E. Asadian, S. Shahrokhian, A. Iraji Zad and F. Ghorbani-Bidkorbeh, *Sensors and Actuators B: Chemical*, 239 (2017) 617
37. P. Lv, X.-W. Tan, K.-H. Yu, R.-L. Zheng, J.-J. Zheng and W. Wei, *Carbon*, 99 (2016) 222
38. J. Zhao, Y. Liu, X. Quan, S. Chen, H. Zhao and H. Yu, *Electrochimica Acta*, 204 (2016) 169